
Operator Learning for Regime-Switching Black–Cox First-Passage Coupled PDE Systems

Anonymous Author(s)

Affiliation

Address

email

Abstract

Regime-switching first-passage-time structural credit models lead to tightly coupled PDEs with absorbing boundaries. Re-solving these PDEs whenever parameters change becomes a key bottleneck for calibration and stress testing, due to high computational cost. To address this, we propose Reflection DeepONet, a physics-informed neural operator whose trunk embeds reflection-principle survival bases to enforce the absorbing boundary by construction, while its branch predicts spectral regime-mixing coefficients from switching intensities. Training is self-supervised by minimizing PDE residuals, using a boundary-robust Huber loss and hybrid sampling that emphasizes the near-maturity boundary layer with gradual regime coupling. Experiments demonstrate robust, consistent regime sensitivity of term structures across single-name, counterparty-risk, and basket settings, enabling fast amortized scenario analysis across a wide range of parameter values.

1 Introduction

Credit risk modeling fundamentally seeks to characterize default timing and survival probabilities within a mathematically consistent framework[9]. This characterization forms the bedrock for asset pricing, risk management, and strategic credit decisions. While reduced-form models offer mathematical tractability by treating default as an exogenous intensity-driven event [4], structural models provide a more transparent link to economic reality. By endogenizing default as the moment a firm’s asset value hits an absorbing boundary—an approach pioneered by Black and Cox [1] and extended to multi-firm correlations by Zhou [15]—first-passage-time (FPT) models offer an intuitive and interpretable mechanism for credit analysis.

Despite their theoretical elegance, extending FPT models to realistic financial environments—such as regime-switching dynamics and multi-firm dependence structures—leads to a rapid escalation in analytical and computational complexity. These extensions give rise to systems of tightly coupled partial differential equations (PDEs) with absorbing boundaries. As demonstrated by Kim et al. [5], solving such systems via traditional finite difference methods is not only computationally expensive but also prone to numerical instabilities near steep boundary gradients. In practical applications such as real-time calibration and large-scale stress testing, where these PDEs must be solved repeatedly over large parameter spaces, classical numerical schemes often become a prohibitive bottleneck.

The emergence of scientific machine learning has introduced a transformative paradigm for addressing these challenges. Physics-Informed Neural Networks (PINNs) [10] embed governing PDEs, boundary conditions, and initial conditions directly into the training objective via automatic differentiation, providing a flexible, mesh-free alternative to classical numerical solvers. PINNs have shown strong performance in high-dimensional financial problems, including complex option pricing and counterparty credit risk modeling [3, 12], and have recently been applied to coupled systems with absorbing barriers, such as barrier option pricing under time-varying interest rates and volatility [2]. Despite

37 these successes, PINNs are fundamentally instance-wise solvers, in the sense that they approximate
 38 solutions for a fixed set of model parameters; consequently, changes in volatilities, regime-switching
 39 intensities, or default boundaries typically require retraining or costly re-optimization. Moreover,
 40 the optimization landscape induced by PDE residual losses becomes particularly challenging in
 41 multi-scale systems or problems with sharp absorbing boundaries, leading to slow convergence and
 42 sensitivity to hyperparameters [2]. Similar limitations are shared by related neural PDE solvers such
 43 as the Deep Galerkin Method (DGM) [11].

44 These limitations have motivated growing interest in operator learning, which aims to learn the
 45 mapping from parameter spaces to solution manifolds for entire families of PDEs, rather than solving
 46 individual instances. Representative frameworks include Deep Operator Networks (DeepONet) [8]
 47 and Fourier Neural Operators (FNO) [7], which have demonstrated that neural models can efficiently
 48 capture parametric solution operators across a wide range of PDE systems. When combined with
 49 physical constraints—through physics-informed operator learning approaches [13]—these models
 50 achieve improved generalization and data efficiency, alleviating the need for repeated retraining
 51 across parameter configurations [14]. This paradigm is particularly well suited to structural credit
 52 modeling, where amortized inference enables rapid generation of survival surfaces across regimes
 53 and market conditions, replacing costly and repetitive numerical simulations.

54 Motivated by these considerations, we propose a physics-informed operator learning framework for
 55 regime-switching first-passage structural credit models. Our approach embeds analytical survival
 56 structure derived from the reflection principle into a neural operator via closed-form marginal survival
 57 bases, providing a structure-aware representation of joint survival. As the model learns the full
 58 mapping from parameters to survival surfaces, it enables rapid evaluation across parameter regimes
 59 and offers an efficient alternative to repeated numerical PDE solvers while preserving financial
 60 interpretability.

61 2 Problem Setting: Regime-Switching First-Passage Survival PDEs

62 2.1 Regime-switching diffusion and default boundaries

63 We consider a two-regime market condition process $Y_t \in \{e_B, e_b\}$ (bull B vs. bear b), modeled
 64 as a continuous-time Markov chain with constant switching intensities $\lambda_B > 0$ (from B to b) and
 65 $\lambda_b > 0$ (from b to B) [5]. The state space is represented by the canonical orthogonal basis vectors
 66 $e_B = (1, 0)^\top$ and $e_b = (0, 1)^\top$ in \mathbb{R}^2 . Under the risk-neutral measure, the asset value $X_i(t)$ of firm
 67 $i = 1, 2$ follows a regime-dependent geometric Brownian motion:

$$dX_i(t) = r^{Y_t} X_i(t) dt + \sigma_i^{Y_t} X_i(t) dW_i(t), \quad dW_1(t)dW_2(t) = \rho dt, \quad (1)$$

68 where r^{Y_t} and $\sigma_i^{Y_t}$ denote the instantaneous risk-free interest rate and the asset return volatility,
 69 respectively, both of which are stochastic processes modulated by the prevailing market regime Y_t .
 70 The stochastic drivers $W_i(t)$ are standard Brownian motions correlated via a constant coefficient
 71 $\rho \in [-1, 1]$, capturing the systematic comovement between the two firms. Default is defined
 72 endogenously as the first passage time $\tau_i(t)$ at which the asset value $X_i(s)$ breaches a time-dependent
 73 solvency barrier $K_i(s)$:

$$\tau_i(t) := \inf\{s \geq t : X_i(s) \leq K_i(s)\}, \quad (2)$$

74 with the barrier typically specified as an exponential function of the form $K_i(s) = K_i e^{\eta_i s}$, where
 75 $K_i > 0$ is a firm-specific constant (the initial solvency barrier level for firm i) and $\eta_i \in \mathbb{R}$ controls
 76 the deterministic growth rate of liabilities [5].

77 2.2 Individual survival PDE system

78 We define the regime-wise survival probability v for firm i (hereafter we focus on firm 1) as

$$v^j(t, x_1) := \mathbb{P}(\tau_1(t) > T \mid X_1(t) = x_1, Y_t = j), \quad j \in \{B, b\}.$$

79 Here, B and b denote the bull and bear regimes, respectively. The underlying regime process Y_t
 80 formally takes values in the canonical basis $\{e_B, e_b\}$; for notational simplicity, we henceforth write
 81 $Y_t = j$ with $j \in \{B, b\}$ instead of $Y_t = e_j$.

82 Then the vector (v^B, v^b) solves a coupled system of absorbing partial differential equations, subject to
 83 the absorbing boundary condition $v^j(t, x) = 0$ for $x \leq K_i(t)$ and the terminal condition $v^j(T, x) =$
 84 $\mathbb{I}(x > K_i(T))$, so survival at maturity occurs if and only if the firm value remains above the barrier.

85 The PDE system is derived via the Feynman–Kac representation for regime-switching diffusions [5,
 86 Eq. 2]:

$$\begin{aligned} \frac{\partial v^B}{\partial t} + r^B x_1 \frac{\partial v^B}{\partial x_1} + \frac{1}{2} (\sigma_1^B x_1)^2 \frac{\partial^2 v^B}{\partial x_1^2} + \lambda_B (v^b - v^B) &= 0, \\ \frac{\partial v^b}{\partial t} + r^b x_1 \frac{\partial v^b}{\partial x_1} + \frac{1}{2} (\sigma_1^b x_1)^2 \frac{\partial^2 v^b}{\partial x_1^2} + \lambda_b (v^B - v^b) &= 0. \end{aligned} \quad (3)$$

87 Here, r^j and σ_1^j denote the regime-dependent interest rate and volatility, respectively, for $j \in \{B, b\}$.

88 2.3 Joint survival PDE system

89 Define the joint regime-wise survival probability for two firms:

$$u^j(t, x_1, x_2) := \mathbb{P}(\tau_1(t) > T, \tau_2(t) > T \mid X_1(t) = x_1, X_2(t) = x_2, Y_t = j).$$

90 Then (u^B, u^b) solves a coupled absorbing PDE system with a cross-derivative term induced by ρ [5,
 91 Eq. 1]:

$$\begin{aligned} \frac{\partial u^B}{\partial t} + r^B \sum_{i=1}^2 x_i \frac{\partial u^B}{\partial x_i} + \sum_{i=1}^2 \frac{1}{2} (\sigma_i^B x_i)^2 \frac{\partial^2 u^B}{\partial x_i^2} \\ + \rho \sigma_1^B \sigma_2^B x_1 x_2 \frac{\partial^2 u^B}{\partial x_1 \partial x_2} + \lambda_B (u^b - u^B) &= 0, \\ \frac{\partial u^b}{\partial t} + r^b \sum_{i=1}^2 x_i \frac{\partial u^b}{\partial x_i} + \sum_{i=1}^2 \frac{1}{2} (\sigma_i^b x_i)^2 \frac{\partial^2 u^b}{\partial x_i^2} \\ + \rho \sigma_1^b \sigma_2^b x_1 x_2 \frac{\partial^2 u^b}{\partial x_1 \partial x_2} + \lambda_b (u^B - u^b) &= 0, \end{aligned} \quad (4)$$

92 2.4 Parameter family and the survival operator

93 Collect coefficients and regime parameters into a compact parameter vector $\Theta \in \Lambda \subset \mathbb{R}^{d_\Theta}$, e.g.,

$$\Theta := (r^B, r^b, \sigma_1^B, \sigma_1^b, \sigma_2^B, \sigma_2^b, \rho, \lambda_B, \lambda_b, \eta_1, \eta_2).$$

94 We define the regime-wise survival operator $\Gamma_{\text{FP}} : \Lambda \rightarrow \mathcal{U}$ as:

$$\Gamma_{\text{FP}}(\Theta)(t, \xi) = U^\Theta(t, \xi) := (U^{B, \Theta}(t, \xi), U^{b, \Theta}(t, \xi))^\top, \quad (5)$$

95 where $\Theta \in \Lambda$ denotes the model parameter vector and U^Θ denotes the corresponding regime-wise
 96 survival function. Here, $\xi = x$ for individual survival and $\xi = (x_1, x_2)$ for joint survival.

97 3 Method: Reflection DeepONet

98 We propose the *Reflection DeepONet*, a physics-informed neural operator architecture designed to
 99 approximate the solution operator Γ_{FP} for the regime-switching survival PDEs (Eqs. 3–4). Unlike
 100 standard finite difference schemes which solve a single instance, our method learns the mapping
 101 from regime intensities $\lambda = [\lambda_B, \lambda_b]^\top$ to the full spatio-temporal survival probability manifolds. We
 102 embed reflection survival bases in the Trunk and learn regime-mixing coefficients in the Branch,
 103 following asymptotics-informed enrichment for residual-based operator learning [6].

104 3.1 Coordinate system and notation

105 **Time-to-maturity.** We work in time-to-maturity coordinates $\tau := T - t$. We denote by $\bar{T} > 0$ the
 106 maximum time-to-maturity considered in training/analysis, so $\tau \in [0, \bar{T}]$.

107 **Log-moneyness relative to the default barrier.** For each firm i , the (time-dependent) barrier is
 108 $K_i(t) = K_i e^{\eta_i t}$ with firm-specific constant $K_i > 0$. We define the barrier-relative log-coordinate

$$z_i := \log\left(\frac{x_i}{K_i(t)}\right),$$

109 so that the default boundary $x_i \leq K_i(t)$ corresponds to $z_i \leq 0$ (absorbing boundary at $z_i = 0$).

110 Equivalently, since $t = T - \tau$, we may write $K_i(T - \tau) = K_i e^{\eta_i(T-\tau)}$ and view $z_i = z_i(\tau)$ when
 111 working in (τ, z) -coordinates.

112 **Spatial variable.** We write $\xi = z \in D_1 := [0, z_{\max}]$ for individual survival and $\xi = (z_1, z_2) \in$
 113 $D_2 \subset \mathbb{R}^2$ for joint survival (both truncated away from infinity). In our experiments we take
 114 $\Omega_z = [0, \ln 3]$, so $D_1 = \Omega_z$ and $D_2 = \Omega_z^2$.

115 **Regime indexing.** The regime process takes values in $\{e_B, e_b\}$, but we write $Y_t = j$ with $j \in$
 116 $\{B, b\}$ for simplicity, and denote the opposite regime by \bar{j} .

117 **Unified survival field.** We denote the regime-wise survival field by $U^\Theta(\tau, \xi) :=$
 118 $(U^{B,\Theta}(\tau, \xi), U^{b,\Theta}(\tau, \xi))^\top$. For clarity, U^Θ corresponds to v^Θ in 1D and u^Θ in 2D in Section 2.

119 3.2 Operator Architecture and Spectral Expansion

120 We approximate the regime-wise survival field $U(\tau, \xi; \lambda) = (U^B(\tau, \xi; \lambda), U^b(\tau, \xi; \lambda))^\top$ using a
 121 modified DeepONet architecture. Here $\xi = z$ for individual survival and $\xi = (z_1, z_2)$ for joint
 122 survival (Section 3.1). The model follows a Branch-Trunk synthesis: the Branch encodes the regime-
 123 switching intensities λ into spectral mixing coefficients, while the Trunk provides a physics-compliant
 124 reflection basis over (τ, ξ) that hard-enforces absorbing boundaries. Throughout, all parameters in Θ
 125 other than λ (e.g., $r^j, \sigma_i^j, \rho, K_i, \eta_i$) are treated as fixed; we learn the operator map $\lambda \mapsto U(\cdot, \cdot; \lambda)$.

126 3.2.1 Branch Network: Parametric Encoder

127 The Branch network, denoted as $\mathcal{N}(\lambda; \theta_{br})$, approximates the mapping from the regime-switching
 128 intensity space $\lambda \subset \Lambda$ to the spectral coefficient space. Its role is to determine the mixing weights of
 129 the basis functions conditional on the market regime.

130 We employ a Multi-Layer Perceptron (MLP) with $L = 3$ hidden layers of width $N_h = 256$. To
 131 ensure higher-order differentiability required for the PDE operators, we use the Sigmoid Linear Unit
 132 (SiLU) activation, denoted by $\text{silu}(\cdot)$:

$$\text{silu}(z) = z \cdot (1 + e^{-z})^{-1}.$$

133 The mapping from the input intensity vector $\lambda = [\lambda_B, \lambda_b]^\top$ to the coefficient vector $\mathbf{c}(\lambda)$ is given by:

$$\begin{aligned} \mathbf{h}_0 &= \lambda, \\ \mathbf{h}_l &= \text{silu}(\mathbf{W}_l \mathbf{h}_{l-1} + \mathbf{b}_l), \quad l = 1, \dots, L, \\ \mathbf{c}(\lambda) &= \mathbf{W}_{\text{out}} \mathbf{h}_L + \mathbf{b}_{\text{out}}. \end{aligned} \tag{6}$$

134 For individual (1D) survival, $\mathbf{c}(\lambda) \in \mathbb{R}^{2M}$ and is reshaped into $\{c_{j,k}(\lambda)\}_{k=1}^M$ for each regime
 135 $j \in \{B, b\}$. For joint (2D) survival, $\mathbf{c}(\lambda) \in \mathbb{R}^{2M^2}$ and is reshaped into $\{c_{j,k,\ell}(\lambda)\}_{k,\ell=1}^M$.

136 3.2.2 Trunk Network: Physics-Informed Reflection Basis

137 Standard neural trunks do not naturally satisfy the absorbing boundary $u(\tau, 0) = 0$. We therefore
 138 build a hard-constrained basis using the reflection principle.

139 **Adaptive Volatility Scaling.** The network learns a spectrum of M effective volatilities to capture
 140 multiscale diffusive behaviors. To distinguish these internal scales from the physical market volatility
 141 σ^{Y_t} and the activation function $\sigma(\cdot)$, we denote the k -th effective diffusivity parameter as $\hat{\sigma}_k$. Since
 142 the raw learnable parameters $\theta_{\sigma,k}$ reside in an unbounded domain ($\theta_{\sigma,k} \in \mathbb{R}$), direct usage could

143 violate the physical constraint of non-negative volatility. To resolve this, we parametrize $\hat{\sigma}_k$ via a
 144 *shifted softplus rectification*:

$$\hat{\sigma}_k = \sigma_{\min} + \ln(1 + \exp(\theta_{\sigma,k})) , \quad k = 1, \dots, M, \quad (7)$$

145 Here $\sigma_{\min} > 0$ ensures strict positivity and numerical stability.

146 This formulation ensures mathematical robustness in two ways. First, the softplus function provides
 147 a smooth, differentiable map from $\mathbb{R} \rightarrow \mathbb{R}^+$, avoiding the non-differentiable points associated
 148 with standard ReLU clipping while ensuring strict positivity. Second, the shift term $\sigma_{\min} = 0.5$
 149 acts as a numerical stabilizer, strictly bounding $\hat{\sigma}_k \geq \sigma_{\min} > 0$ to prevent gradient explosion
 150 caused by division-by-zero in the distance metrics. Here, $\theta_{\sigma,k}$ is a learnable scalar embedded in
 151 the ansatz architecture, distinct from the branch network inputs λ . This decoupling allows the
 152 model to adaptively scale the coordinate distance metrics for each basis function $k \in \{1, \dots, M\}$
 153 independently of the exogenous regime parameters.

154 **Reflection Basis Formulation.** To strictly enforce the structural constraints of the default event, we
 155 construct the k -th basis function $\phi_k(\tau, z; \hat{\sigma}_k)$ using the method of images. This formulation satisfies
 156 the initial condition $\phi_k(0, z) = 1$ for solvent firms ($z > 0$) and the absorbing boundary condition
 157 $\phi_k(\tau, 0) = 0$.

158 Define the effective drift

$$\mu_k = r - \eta - \frac{1}{2}\hat{\sigma}_k^2, \quad (8)$$

159 and the distance metrics

$$d_{1,2}^k(\tau, z) = \frac{\pm z + \mu_k \tau}{\hat{\sigma}_k \sqrt{\tau}}, \quad (9)$$

160 where d_1^k uses $+z$ and d_2^k uses $-z$. The reflection basis is

$$\phi_k(\tau, z; \hat{\sigma}_k) = \begin{cases} 0, & z \leq 0, \\ \Phi(d_1^k) - e^{-\frac{2\mu_k z}{\hat{\sigma}_k^2}} \Phi(d_2^k), & z > 0. \end{cases} \quad (10)$$

161 where $\Phi(\cdot)$ is the standard normal CDF and the exponential term is the reflection factor.

162 **Numerical Enforcement of Hard Constraints.** While the analytical basis theoretically satisfies
 163 the boundary conditions, we strictly enforce these structural constraints in the implementation to
 164 ensure numerical stability.

165 First, the absorbing boundary condition is enforced via an explicit computational mask on the domain:

$$\phi_k(\tau, z; \hat{\sigma}_k) = 0 \quad \text{for } z \leq 0. \quad (11)$$

166 Second, to handle the singularity at $\tau = 0$ (where the term $1/\sqrt{\tau}$ in the distance metrics diverges), we
 167 override the analytical value with the exact initial condition when τ falls below a numerical tolerance
 168 threshold ε :

$$\phi_k(\tau, z; \hat{\sigma}_k) = \mathbb{I}_{\{z>0\}} \quad \text{for } \tau < \varepsilon. \quad (12)$$

169 In our implementation, we set $\varepsilon = 10^{-4}$ to guarantee robust convergence at the maturity boundary.
 170 The effective drift μ_k is determined by the risk-free rate r and the barrier growth rate η : This
 171 formulation ensures correct asymptotics: as $\tau \rightarrow 0$ for $z > 0$, $d_1^k \rightarrow +\infty$ and $d_2^k \rightarrow -\infty$, hence
 172 $\Phi(d_1^k) \rightarrow 1$ and $\Phi(d_2^k) \rightarrow 0$, recovering $\phi_k(0, z) = \mathbb{I}_{\{z>0\}}$.

173 3.2.3 Operator Synthesis: Spectral Expansion in 1D and 2D

174 The approximate solution is constructed as the inner product of the Branch coefficients and the Trunk
 175 reflection basis.

176 **Individual survival (1D).** For each regime $j \in \{B, b\}$, we approximate the marginal survival
 177 probability $v^j(\tau, z)$ by

$$\hat{v}^j(\tau, z; \lambda) = \sum_{k=1}^M c_{j,k}(\lambda) \phi_k(\tau, z; \hat{\sigma}_k). \quad (13)$$

178 **Joint survival (2D).** For each regime $j \in \{B, b\}$, we approximate the joint survival surface
 179 $u^j(\tau, z_1, z_2)$ using a full tensor-product expansion:

$$\hat{u}^j(\tau, z_1, z_2; \boldsymbol{\lambda}) = \sum_{k=1}^M \sum_{l=1}^M c_{j,k,l}(\boldsymbol{\lambda}) \cdot \underbrace{\phi_k^{(1)}(\tau, z_1; \hat{\sigma}_{1,k})}_{\text{Firm 1 Basis}} \cdot \underbrace{\phi_l^{(2)}(\tau, z_2; \hat{\sigma}_{2,l})}_{\text{Firm 2 Basis}}. \quad (14)$$

180 Here $\phi_k^{(1)}$ and $\phi_l^{(2)}$ are the reflection bases for firm 1 and firm 2, respectively, each equipped with its
 181 own learned effective volatility set $\{\hat{\sigma}_{1,k}\}_{k=1}^M$ and $\{\hat{\sigma}_{2,l}\}_{l=1}^M$. The Branch output $\{c_{j,k,l}(\boldsymbol{\lambda})\}$ forms an
 182 interaction tensor that weights cross-terms between the two marginal bases, enabling a non-separable
 183 joint surface.

184 Although each basis factor is one-dimensional, the learned interaction tensor $\{c_{j,k,l}(\boldsymbol{\lambda})\}$ yields
 185 a non-separable approximation of the joint surface under the PDE coupling, with the correlation
 186 parameter ρ treated as fixed in Eq. 4.

187 3.3 Robust Training Objective

188 Let $\boldsymbol{\theta} = \{\theta_{br}, \theta_\sigma\}$ denote the set of all learnable network parameters. We optimize $\boldsymbol{\theta}$ by minimizing
 189 the residuals of the transformed PDE system using Automatic Differentiation (AD) to compute the
 190 exact operators.

191 3.3.1 PDE Residuals in Log-Moneyness Coordinates

192 In the transformed (τ, z) -coordinate system, the backward PDE transforms into a forward parabolic
 193 equation with constant coefficients. The pointwise residual $\mathcal{R}_j(\boldsymbol{\lambda}, \tau, \mathbf{z})$ for regime j is given by:

$$\mathcal{R}_j := \frac{\partial \hat{u}^j}{\partial \tau} - \mathcal{L}_j^{\text{joint}}[\hat{u}^j] - \lambda_j(\hat{u}^{\bar{j}} - \hat{u}^j) \approx 0, \quad (15)$$

194 where \bar{j} denotes the complementary regime. Due to the coordinate transformation, the spatial operator
 195 $\mathcal{L}_j^{\text{joint}}$ simplifies to a constant-coefficient form:

$$\mathcal{L}_j^{\text{joint}}[u] = \sum_{i=1}^2 \left(r^j - \frac{1}{2}(\sigma_i^j)^2 \right) \frac{\partial u}{\partial z_i} + \frac{1}{2} \sum_{i,m=1}^2 \rho_{im} \sigma_i^j \sigma_m^j \frac{\partial^2 u}{\partial z_i \partial z_m}. \quad (16)$$

196 Note that the variable coefficients (e.g., $x \partial_x$) from the original system have been transformed into
 197 constant drift and diffusion terms, which significantly improves the conditioning of the optimization
 198 landscape.

199 3.3.2 Singularity-Robust Loss Function

200 The PDE residuals exhibit numerical instability near the maturity singularity ($\tau \rightarrow 0$). To mitigate
 201 gradient explosions, we employ a Huber Loss \mathcal{H}_δ with threshold $\delta = 0.1$ and a temporal weighting
 202 scheme. The total empirical risk $\mathcal{J}(\boldsymbol{\theta})$ over a batch of N_c collocation points is:

$$\mathcal{J}(\boldsymbol{\theta}) = \frac{1}{N_c} \sum_{i=1}^{N_c} \sum_{j \in \{B, b\}} \left[w_{\text{PDE}}(\tau^{(i)}) \mathcal{H}_\delta(\mathcal{R}_j(\boldsymbol{\lambda}^{(i)}, \tau^{(i)}, \mathbf{z}^{(i)})) + w_{\text{sum}} g(\tau^{(i)}) \mathcal{H}_\delta(\mathcal{R}_j^{\text{sum}}(\boldsymbol{\lambda}^{(i)})) \right], \quad (17)$$

203 where $w_{\text{PDE}}(\tau) := \tanh(5\tau)$ down-weights PDE residuals near $\tau = 0$. To enforce the terminal-scale
 204 normalization only in the near-maturity region, we use a cutoff gate

$$g(\tau) := \mathbb{I}_{\{\tau \leq \tau_{\text{sum}}\}}, \quad \tau_{\text{sum}} = 0.1. \quad (18)$$

205 3.4 Optimization and Discretization

206 **Homotopy Continuation Schedule.** To prevent the high-variance regime-coupling terms from
 207 destabilizing the learning process, we employ a three-phase curriculum learning schedule over the
 208 total 15,000 training epochs:

- **Phase I (Warm-up, Epochs 0–1,000):** We minimize only the terminal-scale normalization penalty to anchor the maturity behavior at $\tau = 0$. The PDE residuals are weighted at zero.
- **Phase II (Ramping, Epochs 1,000–5,000):** We linearly ramp the weights of the PDE residuals and the regime-coupling term from $0 \rightarrow 1$. Concretely, the coupling term $\lambda_j(\hat{u}^j - \hat{u}^j)$ in the residual \mathcal{R}_j is multiplied by a scalar homotopy factor $\alpha(e) = \frac{e-1000}{4000}$, where e is the current epoch.
- **Phase III (Refinement, Epochs 5,000–15,000):** The network trains on the full regime-switching system with constant weights to refine the solution accuracy in the asymptotic region.

Hybrid Domain Sampling. We construct training batches \mathcal{B} using hybrid importance sampling on the time-to-maturity τ :

- **Boundary Layer (20%):** Samples $\tau \sim \mathcal{U}[\varepsilon, 0.1]$ to resolve sharp gradients near the maturity singularity.
- **Asymptotic Region (80%):** Samples $\tau \sim \mathcal{U}[0.1, 10]$ to capture the long-term survival decay.

Spatially, we sample z from the positive domain $\Omega_z = [0, \ln(3.0)]$ (and $(z_1, z_2) \in \Omega_z^2$ for 2D). Since the reflection basis enforces $\hat{u}(\tau, 0) = 0$ by construction, we do not require an explicit boundary collocation set at $z = 0$; instead, we include near-boundary samples through the bulk distribution.

Pricing Integration. Fair CDS spreads are computed by integrating the learned survival profile against the discount factor $D(\tau) = e^{-r\tau}$. We employ a multi-resolution grid that adapts to the solution curvature: an hourly discretization ($\Delta\tau \approx 10^{-4}$) for $\tau \in [0, 0.02]$ to capture short-term jump-to-default risk, and a daily discretization for $\tau > 0.02$. The fair spread s (in basis points) is derived via the discretized risk-neutral valuation formula:

$$s = 10,000 \times \frac{(1-R) \sum_k D(\tau_k) \Delta \hat{u}_k}{\sum_k D(\tau_k) \bar{u}_k \Delta \tau_k}, \quad (19)$$

where $\Delta \hat{u}_k := \hat{u}(\tau_{k-1}) - \hat{u}(\tau_k)$ is the default probability over $(\tau_{k-1}, \tau_k]$, and $\bar{u}_k := \frac{1}{2}(\hat{u}(\tau_{k-1}) + \hat{u}(\tau_k))$ is the interval-average survival probability. For single-name CDS pricing, \hat{u} is taken as the marginal survival estimator (or its regime-mixture, depending on the pricing specification).

4 Numerical Experiments

In this section, we validate the proposed Reflection Deep Operator Network through a series of numerical experiments. We first detail the computational setup and training protocol, demonstrating the method’s efficiency. We then present the main results, focusing on the sensitivity of credit spreads and default correlations to regime-switching intensities (λ_B, λ_b) . Finally, we discuss the quantitative performance and stability of the learned operator.

4.1 Experimental Setup

Implementation and Computational Environment. The framework was implemented in PyTorch and executed on a Google Cloud Platform instance equipped with a single NVIDIA L4 GPU. A significant advantage of the proposed operator learning approach is its memory efficiency; despite the high dimensionality of the joint default problem, the training pipeline required only 2.5 GB of GPU VRAM. This low resource footprint facilitates substantial batch parallelism ($N_{batch} = 4096$) without the need for high-performance computing clusters.

Network Architecture. The neural architecture is designed to enforce physical plausibility by construction. It comprises two coupled networks:

- **Branch Network:** A Multi-Layer Perceptron (MLP) with dimensions [2, 256, 256, 128] that encodes the regime transition parameters $\lambda = (\lambda_B, \lambda_b)$ into a latent coordinate space.

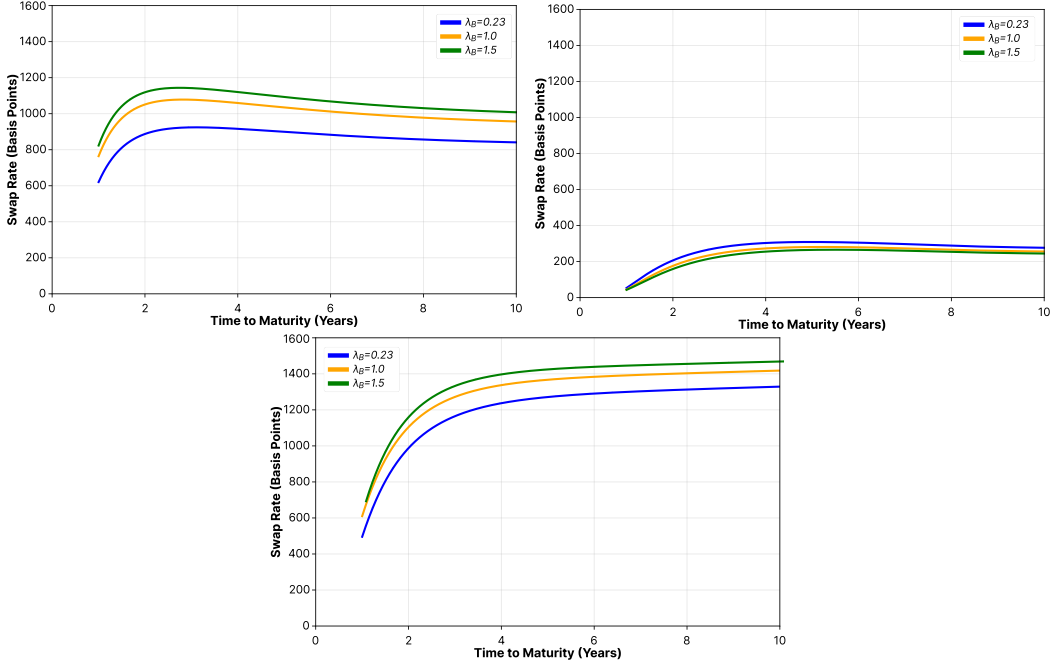


Figure 1: **Regime Sensitivity of Credit Spreads.** **(Top-Left)** Single-Name CDS with a risk-free counterparty shows monotonic sensitivity to instability λ_B . **(Top-Right)** Introduction of Counterparty Default Risk (CDR) compresses spreads and inverts the sensitivity due to bilateral CVA (the Fragile market curve drops below the Stable market curve). **(Bottom)** First-to-Default (FtD) basket spreads are structurally elevated due to weakest-link exposure.

- 252 • **Reflection-Based Trunk:** The trunk provides the reflection basis functions over the
253 spatiotemporal coordinates, and the operator output is formed by a spectral expansion using the
254 Branch coefficients. This construction enforces the absorbing boundary condition by design
255 (in (τ, z) coordinates, the default boundary corresponds to $z = 0$).

256 **Training Protocol.** The optimization involved three independent models: two marginal models for
257 the individual firms (Bank and Corporate) and one joint model for the coupled system. We employed
258 a robust curriculum learning strategy over 15,000 epochs:

- 259 • **Loss Function:** To mitigate gradient explosions near maturity ($\tau \rightarrow 0$), we utilized the
260 Huber loss (Smooth L1) rather than the mean squared error.
261 • **Optimization:** We used the Adam optimizer with an initial learning rate of 10^{-3} , coupled
262 with a Reduce-on-Plateau scheduler (decay factor 0.5, patience 2000).
263 • **Sampling Strategy:** Collocation points were generated in time-to-maturity and log-
264 moneyness coordinates (τ, z) for marginal models and (τ, z_1, z_2) for the joint model, with a
265 higher sampling density near maturity ($\tau < 0.1$) to resolve the boundary layer.

266 **4.2 Main Results: Regime Sensitivity Analysis**

267 To validate the Reflection DeepONet’s ability to generalize across the parameter manifold, we
268 perform a sensitivity analysis on the regime transition intensities. Specifically, we vary the Bull-to-
269 Bear intensity λ_B to test the market’s sensitivity to economic instability, while holding the recovery
270 intensity fixed at $\lambda_b = 1.73$.

271 Crucially, fixing $\lambda_b = 1.73$ implies an expected Bear market duration of $\tau_{bear} = 1/\lambda_b \approx 7$ months,
272 representing a standard recessionary shock that is severe but temporary.

273 **Configuration Details:**

- 274 • **Transition Intensity** (λ_B): We examine three distinct stability regimes:
- 275 1. **Stable Bull Market** ($\lambda_B = 0.23$): The economy is robust, with long expected durations
276 of growth.
- 277 2. **Unstable Bull Market** ($\lambda_B = 1.0$): The economy is volatile, with frequent transitions
278 to distress.
- 279 3. **Fragile Bull Market** ($\lambda_B = 1.5$): The economy is highly precarious; the onset of a
280 recession is imminent.
- 281 • **Market Parameters:** The risk-free rates are set to $r^B = 5\%$ and $r^b = 2\%$. Asset volatilities
282 increase from $\sigma^B = 20\%$ to $\sigma^b = 50\%$ in the Bear regime.

283 Figure 1 presents the term structure of fair spreads for three distinct credit instruments generated by
284 the operator under these regimes.

285 **Single-Name CDS (Risk-Free Counterparty).** As shown in the **top-left panel**, spreads widen
286 monotonically as the market becomes more fragile ($\lambda_B = 1.5$ vs. $\lambda_B = 0.23$). This reflects the
287 heightened probability of transitioning into the high-volatility Bear regime. The term structure exhibits
288 a characteristic "hump" at intermediate maturities (3–5 years), indicating that regime uncertainty
289 commands the largest risk premium over medium-term horizons before mean-reverting.

290 **Impact of Counterparty Default Risk (CDR).** The **top-right panel** reveals a significant structural
291 shift when the protection seller is correlated with the underlying asset. The spread levels are drastically
292 compressed compared to the risk-free case. Notably, the sensitivity to λ_B *inverts*: the "Fragile"
293 market curve drops below the "Stable" market curve. This is because, in a fragile economy, the
294 probability of the insurer defaulting rises simultaneously with the asset's risk. This *Wrong-Way Risk*
295 renders the protection less valuable in the exact states where it is needed most, forcing a discount on
296 the fair premium.

297 **Basket Default Swap (First-to-Default).** In the **bottom panel**, the First-to-Default (FtD) spreads
298 are structurally elevated, peaking above 1400 bps. This reflects the "weakest-link" mechanics
299 ($\tau_{\text{FtD}} = \min(\tau_1, \tau_2)$), where risk is effectively additive. While spreads still rise with instability λ_B ,
300 the marginal widening is partially dampened by correlation saturation in the Bear regime, where
301 clustered defaults limit the payout to a single event.

302 Overall, the operator correctly captures the non-linear interplay between regime instability and
303 contract structure, consistent with the theoretical first-passage-time implications reported by Kim
304 et al. [5].

305 5 Conclusion

306 We propose a self-supervised, boundary-aware neural operator that amortizes the solution of regime-
307 switching first-passage coupled PDEs over parameter families, replacing repeated numerical solves
308 with fast inference once training is complete. Beyond computational speedups, the operator-learning
309 perspective provides a unified lens for analyzing how regime dynamics and cross-firm dependence
310 propagate through first-passage default mechanisms, facilitating sensitivity analysis, scenario explo-
311 ration, and stress testing at scale.

312 Our approach amortizes the solution of regime-switching first-passage coupled PDEs with a self-
313 supervised neural operator, enabling efficient term-structure analysis across parameter families;
314 however, several limitations remain. The regime specification is intentionally stylized, focusing
315 on a two-state Markov chain with constant switching intensities, which may not capture richer
316 time- or state-dependent regime dynamics. Moreover, the diffusion-based structural setting with
317 absorbing default boundaries, while interpretable, may be restrictive in applications where jumps,
318 stochastic volatility, or more flexible dependence structures are important. We also do not yet report a
319 systematic quantitative benchmark against high-accuracy finite-difference (FDM) solutions across
320 broad parameter sweeps.

321 Future work will therefore extend the regime process to multi-state and time/state-dependent trans-
322 sitions, broaden the structural dynamics beyond pure diffusions, and integrate the operator into
323 calibration workflows that link amortized survival surfaces to market observables and parameter
324 inference.

325 **References**

- 326 [1] Fischer Black and John C. Cox. Valuing corporate securities: Some effects of bond indenture
327 provisions. *The Journal of Finance*, 31(2):351–367, 1976.
- 328 [2] Yu Chen, Xing Lü, Hao Tian, and Rui-Heng Li. Physics-informed neural network for barrier
329 option pricing in coupled financial quantitative systems with varying interest rate and volatility.
330 *Engineering Analysis with Boundary Elements*, 180:106457, 2025. doi: 10.1016/j.enganabound.
331 2025.106457.
- 332 [3] Yu Chen, Xing L"u, Hao Tian, and Rui-Heng Li. Physics-informed neural network for barrier
333 option pricing in coupled financial quantitative system with varying interest rate and volatility.
334 *Engineering Analysis with Boundary Elements*, 180:106457, 2025.
- 335 [4] Darrell Duffie and Kenneth J. Singleton. Modeling term structures of defaultable bonds. *Review
336 of Financial Studies*, 12(4):687–720, 1999.
- 337 [5] In Joon Kim, Jaewoo Jang, and Seung Jin Lee. A first-passage-time model under regime-
338 switching market environment. *Journal of Economic Dynamics and Control*, 32(10):3304–3328,
339 2008.
- 340 [6] Jinsil Lee, Youngjoon Hong, Seungchan Ko, and Jae Yong Lee. Data-free asymptotics-informed
341 operator networks for singularly perturbed pdes. *arXiv preprint arXiv:2512.22006*, 2025.
- 342 [7] Zongyi Li, Nikola Kovachki, Kamyar Azizzadenesheli, Burigede Liu, Kaushik Bhattacharya,
343 Andrew Stuart, and Anima Anandkumar. Fourier neural operator for parametric partial differen-
344 tial equations. In *International Conference on Learning Representations (ICLR)*, 2021.
- 345 [8] Lu Lu, Pengzhan Jin, and George E. Karniadakis. Learning nonlinear operators via deeponet
346 based on the universal approximation theorem of operators. *Nature Machine Intelligence*, 3(3):
347 218–229, 2021.
- 348 [9] Robert C Merton. On the pricing of corporate debt: The risk structure of interest rates. *The
349 Journal of finance*, 29(2):449–470, 1974.
- 350 [10] Maziar Raissi, Paris Perdikaris, and George E. Karniadakis. Physics-informed neural networks:
351 A deep learning framework for solving forward and inverse problems involving nonlinear
352 partial differential equations. *Journal of Computational Physics*, 378:686–707, 2019. doi:
353 10.1016/j.jcp.2018.10.045.
- 354 [11] Justin Sirignano and Konstantinos Spiliopoulos. Dgm: A deep learning algorithm for solving
355 partial differential equations. *Journal of Computational Physics*, 375:1339–1364, 2018.
- 356 [12] Joel P. Villarino, Álvaro Leitão, and José A. García-Rodríguez. Boundary-safe pinns exten-
357 sion: Application to non-linear parabolic pdes in counterparty credit risk. *arXiv preprint
358 arXiv:2210.02175*, 2022.
- 359 [13] Sifan Wang, Hanwen Wang, and Paris Perdikaris. Learning the solution operator of parametric
360 partial differential equations with physics-informed deeponets. *Science Advances*, 7(40):
361 eabi8605, 2021.
- 362 [14] Zhiwei Xu, Zongyi Zhang, and George E. Karniadakis. Data-free asymptotics-informed operator
363 networks for singularly perturbed partial differential equations. *Journal of Computational
364 Physics*, 473:111746, 2023.
- 365 [15] Chunsheng Zhou. An analysis of default correlations and multiple defaults. *Review of Financial
366 Studies*, 14(2):555–576, 2001.

367 **AI Co-Scientist Challenge Korea Paper Checklist**

368 **1. Claims**

369 Question: Do the main claims made in the abstract and introduction accurately reflect the
370 paper's contributions and scope?

371 Answer: [Yes]

372 Justification: The abstract and introduction propose a physics-informed operator for regime-
373 switching PDEs. Section 3 details the Reflection DeepONet architecture, and Section 4
374 validates its ability to capture regime sensitivities in credit spreads as claimed.

375 Guidelines:

- 376 • The answer NA means that the abstract and introduction do not include the claims
377 made in the paper.
- 378 • The abstract and/or introduction should clearly state the claims made, including the
379 contributions made in the paper and important assumptions and limitations. A No or
380 NA answer to this question will not be perceived well by the reviewers.
- 381 • The claims made should match theoretical and experimental results, and reflect how
382 much the results can be expected to generalize to other settings.
- 383 • It is fine to include aspirational goals as motivation as long as it is clear that these goals
384 are not attained by the paper.

385 **2. Limitations**

386 Question: Does the paper discuss the limitations of the work performed by the authors?

387 Answer: [Yes]

388 Justification: In the "Limitation and future work" section, we explicitly discuss the stylized
389 two-state regime assumption, the restriction to diffusion-based structural dynamics, and the
390 current lack of end-to-end market calibration.

391 Guidelines:

- 392 • The answer NA means that the paper has no limitation while the answer No means that
393 the paper has limitations, but those are not discussed in the paper.
- 394 • The authors are encouraged to create a separate "Limitations" section in their paper.
- 395 • The paper should point out any strong assumptions and how robust the results are to
396 violations of these assumptions (e.g., independence assumptions, noiseless settings,
397 model well-specification, asymptotic approximations only holding locally). The authors
398 should reflect on how these assumptions might be violated in practice and what the
399 implications would be.
- 400 • The authors should reflect on the scope of the claims made, e.g., if the approach was
401 only tested on a few datasets or with a few runs. In general, empirical results often
402 depend on implicit assumptions, which should be articulated.
- 403 • The authors should reflect on the factors that influence the performance of the approach.
404 For example, a facial recognition algorithm may perform poorly when image resolution
405 is low or images are taken in low lighting. Or a speech-to-text system might not be
406 used reliably to provide closed captions for online lectures because it fails to handle
407 technical jargon.
- 408 • The authors should discuss the computational efficiency of the proposed algorithms
409 and how they scale with dataset size.
- 410 • If applicable, the authors should discuss possible limitations of their approach to
411 address problems of privacy and fairness.
- 412 • While the authors might fear that complete honesty about limitations might be used by
413 reviewers as grounds for rejection, a worse outcome might be that reviewers discover
414 limitations that aren't acknowledged in the paper. The authors should use their best
415 judgment and recognize that individual actions in favor of transparency play an impor-
416 tant role in developing norms that preserve the integrity of the community. Reviewers
417 will be specifically instructed to not penalize honesty concerning limitations.

418 **3. Theory Assumptions and Proofs**

419 Question: For each theoretical result, does the paper provide the full set of assumptions and
420 a complete (and correct) proof?

421 Answer: [Yes]

422 Justification: Section 2 clearly defines the stochastic assumptions (regime-switching GBM)
423 and the coupled PDE system. The Reflection Principle construction in Section 3 is derived
424 from standard analytical results for Brownian motion.

425 Guidelines:

- 426 • The answer NA means that the paper does not include theoretical results.
- 427 • All the theorems, formulas, and proofs in the paper should be numbered and cross-
428 referenced.
- 429 • All assumptions should be clearly stated or referenced in the statement of any theorems.
- 430 • The proofs can either appear in the main paper or the supplemental material, but if
431 they appear in the supplemental material, the authors are encouraged to provide a short
432 proof sketch to provide intuition.
- 433 • Inversely, any informal proof provided in the core of the paper should be complemented
434 by formal proofs provided in appendix or supplemental material.
- 435 • Theorems and Lemmas that the proof relies upon should be properly referenced.

436 4. Experimental Result Reproducibility

437 Question: Does the paper fully disclose all the information needed to reproduce the main ex-
438 perimental results of the paper to the extent that it affects the main claims and/or conclusions
439 of the paper (regardless of whether the code and data are provided or not)?

440 Answer: [Yes]

441 Justification: Section 3.3 details the 15,000-epoch curriculum schedule and sampling strategy.
442 Section 4.1 specifies the network architecture, optimizer settings (Adam), and batch size
443 used to generate the results.

444 Guidelines:

- 445 • The answer NA means that the paper does not include experiments.
- 446 • If the paper includes experiments, a No answer to this question will not be perceived
447 well by the reviewers: Making the paper reproducible is important, regardless of
448 whether the code and data are provided or not.
- 449 • If the contribution is a dataset and/or model, the authors should describe the steps taken
450 to make their results reproducible or verifiable.
- 451 • Depending on the contribution, reproducibility can be accomplished in various ways.
452 For example, if the contribution is a novel architecture, describing the architecture fully
453 might suffice, or if the contribution is a specific model and empirical evaluation, it may
454 be necessary to either make it possible for others to replicate the model with the same
455 dataset, or provide access to the model. In general, releasing code and data is often
456 one good way to accomplish this, but reproducibility can also be provided via detailed
457 instructions for how to replicate the results, access to a hosted model (e.g., in the case
458 of a large language model), releasing of a model checkpoint, or other means that are
459 appropriate to the research performed.
- 460 • While AI Co-Scientist Challenge Korea does not require releasing code, the conference
461 does require all submissions to provide some reasonable avenue for reproducibility,
462 which may depend on the nature of the contribution. For example
 - 463 (a) If the contribution is primarily a new algorithm, the paper should make it clear how
464 to reproduce that algorithm.
 - 465 (b) If the contribution is primarily a new model architecture, the paper should describe
466 the architecture clearly and fully.
 - 467 (c) If the contribution is a new model (e.g., a large language model), then there should
468 either be a way to access this model for reproducing the results or a way to reproduce
469 the model (e.g., with an open-source dataset or instructions for how to construct
470 the dataset).

471 (d) We recognize that reproducibility may be tricky in some cases, in which case
472 authors are welcome to describe the particular way they provide for reproducibility.
473 In the case of closed-source models, it may be that access to the model is limited in
474 some way (e.g., to registered users), but it should be possible for other researchers
475 to have some path to reproducing or verifying the results.

476 **5. Open access to data and code**

477 Question: Does the paper provide open access to the data and code, with sufficient instruc-
478 tions to faithfully reproduce the main experimental results, as described in supplemental
479 material?

480 Answer: [No]

481 Justification: We plan to release the full source code and reproduction scripts upon accep-
482 tance of the paper. All experimental details (architecture, hyperparameters, sampling) are
483 fully described in Section 4 to ensure reproducibility in the interim.

484 Guidelines:

- 485 • The answer NA means that paper does not include experiments requiring code.
- 486 • Please see the NeurIPS code and data submission guidelines (<https://nips.cc/public/guides/CodeSubmissionPolicy>) for more details.
- 487 • While we encourage the release of code and data, we understand that this might not be
488 possible, so “No” is an acceptable answer. Papers cannot be rejected simply for not
489 including code, unless this is central to the contribution (e.g., for a new open-source
490 benchmark).
- 491 • The instructions should contain the exact command and environment needed to run to
492 reproduce the results. See the NeurIPS code and data submission guidelines (<https://nips.cc/public/guides/CodeSubmissionPolicy>) for more details.
- 493 • The authors should provide instructions on data access and preparation, including how
494 to access the raw data, preprocessed data, intermediate data, and generated data, etc.
- 495 • The authors should provide scripts to reproduce all experimental results for the new
496 proposed method and baselines. If only a subset of experiments are reproducible, they
497 should state which ones are omitted from the script and why.
- 498 • At submission time, to preserve anonymity, the authors should release anonymized
499 versions (if applicable).
- 500 • Providing as much information as possible in supplemental material (appended to the
501 paper) is recommended, but including URLs to data and code is permitted.

504 **6. Experimental Setting/Details**

505 Question: Does the paper specify all the training and test details (e.g., data splits, hyper-
506 parameters, how they were chosen, type of optimizer, etc.) necessary to understand the
507 results?

508 Answer: [Yes]

509 Justification: Section 4.1 specifies the hyperparameters (Learning Rate 10^{-3} , Batch Size
510 4096), the Scheduler (Reduce-on-Plateau), and the domain sampling strategy.

511 Guidelines:

- 512 • The answer NA means that the paper does not include experiments.
- 513 • The experimental setting should be presented in the core of the paper to a level of detail
514 that is necessary to appreciate the results and make sense of them.
- 515 • The full details can be provided either with the code, in appendix, or as supplemental
516 material.

517 **7. Experiment Statistical Significance**

518 Question: Does the paper report error bars suitably and correctly defined or other appropriate
519 information about the statistical significance of the experiments?

520 Answer: [No]

521 Justification: The results focus on a regime sensitivity analysis to demonstrate financial
522 plausibility (monotonicity, term structure) rather than aggregated statistical performance
523 metrics. A detailed quantitative benchmark against FDM is described as ongoing work.

524 Guidelines:

- The answer NA means that the paper does not include experiments.
- The authors should answer "Yes" if the results are accompanied by error bars, confidence intervals, or statistical significance tests, at least for the experiments that support the main claims of the paper.
- The factors of variability that the error bars are capturing should be clearly stated (for example, train/test split, initialization, random drawing of some parameter, or overall run with given experimental conditions).
- The method for calculating the error bars should be explained (closed form formula, call to a library function, bootstrap, etc.)
- The assumptions made should be given (e.g., Normally distributed errors).
- It should be clear whether the error bar is the standard deviation or the standard error of the mean.
- It is OK to report 1-sigma error bars, but one should state it. The authors should preferably report a 2-sigma error bar than state that they have a 96% CI, if the hypothesis of Normality of errors is not verified.
- For asymmetric distributions, the authors should be careful not to show in tables or figures symmetric error bars that would yield results that are out of range (e.g. negative error rates).
- If error bars are reported in tables or plots, The authors should explain in the text how they were calculated and reference the corresponding figures or tables in the text.

545 **8. Experiments Compute Resources**

546 Question: For each experiment, does the paper provide sufficient information on the
547 computer resources (type of compute workers, memory, time of execution) needed to reproduce
548 the experiments?

549 Answer: [Yes]

550 Justification: Section 4.1 explicitly states the experiments were run on a Google Cloud
551 Platform instance with a single NVIDIA L4 GPU, using approximately 2.5 GB of VRAM.

552 Guidelines:

- The answer NA means that the paper does not include experiments.
- The paper should indicate the type of compute workers CPU or GPU, internal cluster, or cloud provider, including relevant memory and storage.
- The paper should provide the amount of compute required for each of the individual experimental runs as well as estimate the total compute.
- The paper should disclose whether the full research project required more compute than the experiments reported in the paper (e.g., preliminary or failed experiments that didn't make it into the paper).

561 **9. Code Of Ethics**

562 Question: Does the research conducted in the paper conform, in every respect, with the
563 NeurIPS Code of Ethics <https://nips.cc/public/EthicsGuidelines>?

564 Answer: [Yes]

565 Justification: The research involves mathematical modeling of financial derivatives. We
566 have reviewed the code of ethics and found no conflicts.

567 Guidelines:

- The answer NA means that the authors have not reviewed the NeurIPS Code of Ethics.
- If the authors answer No, they should explain the special circumstances that require a deviation from the Code of Ethics.
- The authors should make sure to preserve anonymity (e.g., if there is a special consideration due to laws or regulations in their jurisdiction).

573 **10. Broader Impacts**

574 Question: Does the paper discuss both potential positive societal impacts and negative
575 societal impacts of the work performed?

576 Answer: [Yes]

577 Justification: The work contributes to more accurate financial risk management (positive).
578 We acknowledge the general model risk associated with deploying AI in regulated financial
579 sectors (negative/cautionary).

580 Guidelines:

- 581 • The answer NA means that there is no societal impact of the work performed.
- 582 • If the authors answer NA or No, they should explain why their work has no societal
583 impact or why the paper does not address societal impact.
- 584 • Examples of negative societal impacts include potential malicious or unintended uses
585 (e.g., disinformation, generating fake profiles, surveillance), fairness considerations
586 (e.g., deployment of technologies that could make decisions that unfairly impact specific
587 groups), privacy considerations, and security considerations.
- 588 • The conference expects that many papers will be foundational research and not tied
589 to particular applications, let alone deployments. However, if there is a direct path to
590 any negative applications, the authors should point it out. For example, it is legitimate
591 to point out that an improvement in the quality of generative models could be used to
592 generate deepfakes for disinformation. On the other hand, it is not needed to point out
593 that a generic algorithm for optimizing neural networks could enable people to train
594 models that generate Deepfakes faster.
- 595 • The authors should consider possible harms that could arise when the technology is
596 being used as intended and functioning correctly, harms that could arise when the
597 technology is being used as intended but gives incorrect results, and harms following
598 from (intentional or unintentional) misuse of the technology.
- 599 • If there are negative societal impacts, the authors could also discuss possible mitigation
600 strategies (e.g., gated release of models, providing defenses in addition to attacks,
601 mechanisms for monitoring misuse, mechanisms to monitor how a system learns from
602 feedback over time, improving the efficiency and accessibility of ML).

603 **11. Safeguards**

604 Question: Does the paper describe safeguards that have been put in place for responsible
605 release of data or models that have a high risk for misuse (e.g., pretrained language models,
606 image generators, or scraped datasets)?

607 Answer: [N/A]

608 Justification: The proposed model is a PDE solver for credit risk and does not involve
609 high-risk generative capabilities or personal data.

610 Guidelines:

- 611 • The answer NA means that the paper poses no such risks.
- 612 • Released models that have a high risk for misuse or dual-use should be released with
613 necessary safeguards to allow for controlled use of the model, for example by requiring
614 that users adhere to usage guidelines or restrictions to access the model or implementing
615 safety filters.
- 616 • Datasets that have been scraped from the Internet could pose safety risks. The authors
617 should describe how they avoided releasing unsafe images.
- 618 • We recognize that providing effective safeguards is challenging, and many papers do
619 not require this, but we encourage authors to take this into account and make a best
620 faith effort.

621 **12. Licenses for existing assets**

622 Question: Are the creators or original owners of assets (e.g., code, data, models), used in
623 the paper, properly credited and are the license and terms of use explicitly mentioned and
624 properly respected?

625 Answer: [Yes]

626 Justification: We use standard open-source libraries (e.g., PyTorch) which are properly cited.

627 Guidelines:

- 628 • The answer NA means that the paper does not use existing assets.

- 629 • The authors should cite the original paper that produced the code package or dataset.
630 • The authors should state which version of the asset is used and, if possible, include a
631 URL.
632 • The name of the license (e.g., CC-BY 4.0) should be included for each asset.
633 • For scraped data from a particular source (e.g., website), the copyright and terms of
634 service of that source should be provided.
635 • If assets are released, the license, copyright information, and terms of use in the
636 package should be provided. For popular datasets, paperswithcode.com/datasets
637 has curated licenses for some datasets. Their licensing guide can help determine the
638 license of a dataset.
639 • For existing datasets that are re-packaged, both the original license and the license of
640 the derived asset (if it has changed) should be provided.
641 • If this information is not available online, the authors are encouraged to reach out to
642 the asset's creators.

643 **13. New Assets**

644 Question: Are new assets introduced in the paper well documented and is the documentation
645 provided alongside the assets?

646 Answer: [No]

647 Justification: We are not releasing new assets (code, models, or datasets) at the time of
648 submission.

649 Guidelines:

- 650 • The answer NA means that the paper does not release new assets.
651 • Researchers should communicate the details of the dataset/code/model as part of their
652 submissions via structured templates. This includes details about training, license,
653 limitations, etc.
654 • The paper should discuss whether and how consent was obtained from people whose
655 asset is used.
656 • At submission time, remember to anonymize your assets (if applicable). You can either
657 create an anonymized URL or include an anonymized zip file.

658 **14. Crowdsourcing and Research with Human Subjects**

659 Question: For crowdsourcing experiments and research with human subjects, does the paper
660 include the full text of instructions given to participants and screenshots, if applicable, as
661 well as details about compensation (if any)?

662 Answer: [N/A]

663 Justification: The research does not involve human subjects.

664 Guidelines:

- 665 • The answer NA means that the paper does not involve crowdsourcing nor research with
666 human subjects.
667 • Including this information in the supplemental material is fine, but if the main contribu-
668 tion of the paper involves human subjects, then as much detail as possible should be
669 included in the main paper.
670 • According to the NeurIPS Code of Ethics, workers involved in data collection, curation,
671 or other labor should be paid at least the minimum wage in the country of the data
672 collector.

673 **15. Institutional Review Board (IRB) Approvals or Equivalent for Research with Human
674 Subjects**

675 Question: Does the paper describe potential risks incurred by study participants, whether
676 such risks were disclosed to the subjects, and whether Institutional Review Board (IRB)
677 approvals (or an equivalent approval/review based on the requirements of your country or
678 institution) were obtained?

679 Answer: [N/A]

680 Justification: The research does not involve human subjects.

681

Guidelines:

682

- The answer NA means that the paper does not involve crowdsourcing nor research with human subjects.
- Depending on the country in which research is conducted, IRB approval (or equivalent) may be required for any human subjects research. If you obtained IRB approval, you should clearly state this in the paper.
- We recognize that the procedures for this may vary significantly between institutions and locations, and we expect authors to adhere to the NeurIPS Code of Ethics and the guidelines for their institution.
- For initial submissions, do not include any information that would break anonymity (if applicable), such as the institution conducting the review.

683

684

685

686

687

688

689

690

691